Simulation of reactive solute transport in the critical zone: A Lagrangian model for transient flow and preferential transport

Alexander Sternagel[1], Ralf Loritz[1], Julian Klaus[2], Brian Berkowitz[3], Erwin Zehe[1]

[1] Karlsruhe Institute of Technology (KIT), Institute of Water Resources and River Basin Management, Hydrology, Germany
[2] Luxembourg Institute of Science and Technology (LIST), Environmental Research and Innovation Department, Catchment and Eco-Hydrology Research Group, Luxembourg
[3] Department of Earth and Planetary Sciences, Weizmann Institute of Science, Israel

Correspondence to: Alexander Sternagel (alexander.sternagel@kit.edu)

Abstract. We present an approach to simulate reactive solute transport within the Lagrangian Soil Water and Solute Transport Model framework (LAST). The LAST-Model employs a Lagrangian perspective to describe the (1-D) movement of discrete water particles, which travel at different velocities and carry solutes through a heterogeneous, partially saturated soil that is subdivided into a soil matrix and structural macropore domain.

In this study, we implement an approach to represent non-linear sorption and first-order degradation processes of reactive solutes under well-mixed and preferential flow conditions in the critical zone. The intensity of the two reactive transport processes may vary with the soil depth, to account for topsoil that facilitates enhanced microbial activity (and hence sorption) as well as chemical turnover rates. This expanded LAST-Model is evaluated with simulations of conservative tracer transport and reactive transport of the herbicide Isoproturon, at different flow conditions, and compared to data from field experiments. Additionally, the model is compared to simulations from the commonly used HYDRUS 1-D model. Both models show equal performance at a matrix flow dominated site, but LAST better matches indicators of preferential flow at a macropore flow dominated site. These results demonstrate the feasibility of the approach to simulate reactive transport in the LAST-Model framework, and highlight the advantage of the structural macropore domain to cope with preferential bypassing of topsoil and subsequent re-infiltration into the subsoil matrix.

1 Introduction

Reactive substances like pesticides are subject to chemical reactions within the critical zone (Kutílek and Nielsen, 1994; Fomsgaard, 1995). Their mobility and life span depend greatly on various factors like (i) the spectrum of transport velocities, (ii) the sorption to soil materials (Knabner et al., 1996) and (iii) microbial degradation and turnover (cf. Sect. 3). The multitude and complexity of these factors are a considerable source of uncertainty in pesticide fate modelling, as it is still not fully understood how pesticides are transported within different soils and particularly how preferential flow through macropores impacts the breakthrough of these substances into streams and groundwater (e.g. Flury, 1996; Arias-Estévez et al., 2008; Frey et al., 2009; Klaus et al., 2014).

To advance our understanding of reactive solute transport (RT) of pesticides, particularly the joint controls of macropores, sorption and degradation, a combination of predictive models and plot-scale experiments is often used (e.g. Zehe et al., 2001; Simunek et al., 2008; Radcliffe and Simunek, 2010; Klaus and Zehe, 2011; Klaus et al., 2013). Such methods can be used subsequently to evaluate the environmental risks related to the wide use of reactive substances (Pimentel et al., 1992; Carter, 2000; Gill and Garg, 2014; Liess et al., 1999). Combining the

Richards and advection-dispersion equations is one common approach used to simulate water flow dynamics and (reactive) solute transport in the partially saturated soil zone. This approach has been implemented, for example, in the well-established models HYDRUS (Gerke and van Genuchten, 1993; Simunek et al., 2008), MACRO (Jarvis and Larsbo, 2012) and Zin AgriTra (Gassmann et al., 2013). However, this approach has well-known deficiencies

5 in simulating preferential macropore flow and imperfect mixing with the matrix in the vadose zone (Beven and Germann, 2013). As both processes essentially control environmental risk due to transport of reactive substances, a range of adaptions has been proposed to improve this deficiency (Šimůnek et al., 2003). One frequently-used adaption is the dual-domain concept, which describes matrix and macropore flow in separated, exchanging continua to account for local disequilibrium conditions (Gerke, 2006). However, studies show that even these dual-

10 domain models can be insufficient to quantify preferential solute breakthrough into the subsoil (Sternagel et al., 2019) or into tile drains (Haws et al., 2005; Köhne et al., 2009b, a). A different approach is to represent macropores as spatially connected, highly permeable flow paths in the same domain as the soil matrix (Sander and Gerke, 2009). This concept has been shown to operate well for preferential flow of water and bromide tracers at a forested hillslope (Wienhöfer and Zehe, 2014), and for bromide and Isoproturon transport through worm burrows into a

15 tile drain at a field site (Klaus and Zehe, 2011). Nevertheless, this approach is based on the Richards equation and is thus limited to laminar flow conditions with sufficiently small flow velocities corresponding to a Reynolds number smaller 10 (Loritz et al., 2017).

Particle-based approaches offer a promising alternative to simulate reactive transport. These approaches work with a Lagrangian perspective on the movement of solute particles in a flow field, rather than solving the advection-

20 dispersion equation directly. They have been particularly effective in quantifying solute transport alone, while the movement of the fluid carrying solutes is still usually integrated in systems based on Eulerian control volumes (e.g. Delay and Bodin, 2001; Zehe et al., 2001; Berkowitz et al., 2006; Koutsoyiannis, 2010; Klaus and Zehe, 2010). In the context of saturated flow in fractured and heterogeneous aquifers, Lagrangian descriptions of fluid flow are already commonly and successfully applied. For example, the Continuous Time Random Walk (CTRW)

25 approach accounts for non-Fickian transport of tracer particles within the water flow through heterogeneous, geological formations via different flow paths with an associated distribution of velocities and thus travel times (Berkowitz et al., 2006; Berkowitz et al., 2016; Hansen and Berkowitz, 2020). However, Lagrangian modelling of fluid flow in the vadose zone is more challenging due to the dependence of the velocity field on the temporally changing soil moisture states and boundary conditions. This explains why only a relatively small number of models

30 use Lagrangian approaches for solute transport, and also for water particles (also called water "parcels") to characterize the fluid phase itself (e.g. Ewen, 1996a, b; Bücker-Gittel et al., 2003; Davies and Beven, 2012; Zehe and Jackisch, 2016; Jackisch and Zehe, 2018). Sternagel et al. (2019) proposed that these water particles may optionally carry solute masses to simulate non-reactive transport. Their Lagrangian Soil Water and Solute Transport Model (LAST) combines the assets of the Lagrangian approach with an Euler-Grid to simulate fluid

35 motion and solute transport in heterogeneous, partially saturated 1-D soil domains. It allows discrete water particles to travel at different velocities and carry temporally-variable solute masses through the subsurface domain. The soil domain is subdivided into a soil matrix and a structurally defined preferential flow/macropore domain (cf. Sect. 2). A comparison of HYDRUS 1-D and the LAST-Model based on plot scale tracer experiments showed that both models perform similarly in case of matrix flow dominated tracer transport; however, under preferential flow

40 conditions, LAST better matched observed tracer profiles indicating preferential flow (Sternagel et al., 2019).

While the results of Sternagel et al. (2019) demonstrate the feasibility of the Lagrangian approach to simulate conservative tracer transport even under preferential flow conditions during one-day simulations, a generalization of the Lagrangian approach to reactive solute transport and larger time scales is still missing. In this context it is important to recall that the use of spatially discrete control volumes (Euler-Grids) to calculate concentrations of water and solute particles in Lagrangian models can suffer from the problem of artificial over-mixing (e.g. Boso et al., 2013; Cui et al., 2014; e.g. Berkowitz et al., 2016; Benson et al., 2017). This is because water and solutes are assumed to mix perfectly within the elements of such an Euler-Grid, which may lead to a smoothing of gradients in the case of coarse grid sizes. This might lead to overestimates of concentration dilution while solutes infiltrate into and distribute within the soil domain (Green et al., 2002).

The main objectives of this study are thus to

1. develop an approach to represent reactive transport, i.e., sorption and degradation of solutes within the Lagrangian framework under well-mixed and preferential flow conditions and implement this into the LAST-Model. We test the feasibility of the approach by simulating plot-scale experiments with a bromide tracer and the herbicide Isoproturon (IPU) (Zehe and Flühler, 2001), and use corresponding simulations of the commonly applied model HYDRUS 1-D as a benchmark;

2. perform long-term simulations to explore the reactive transport behaviour with LAST on larger time scales. This will additionally shed light on the susceptibility of the LAST-Model to artificial over-mixing of solutes in the Euler-Grid. For this purpose, we make use of bromide data from irrigation experiments (Klaus et al., 2014).

2 The LAST-Model: Concept, theoretical background and numerical implementation

2.1 Model concept

The LAST-Model combines a Lagrangian approach with an Euler-Grid to simulate fluid motion and solute transport in heterogeneous, partially saturated 1-D soil domains. Discrete water particles with a constant water mass and volume carry temporally-variable information about their position and solute concentrations through defined domains for soil matrix and macropores that are subdivided into vertical grid elements (Euler-Grid). In these grid elements, the water particle density represents the soil water content (Zehe and Jackisch, 2016) and particles are assumed to be stored in soil pores of different sizes. As a function of this pore size distribution, particles travel with different velocities (cf. Fig. 1). Particle movements are thus determined by the actual hydraulic conductivity and water diffusivity in combination with a spatial random walk (cf. Sect. 2.2, Eq. 5). This approach represents the joint effects of gravity and capillary forces on water flow in partially saturated soils. The use of an Euler-Grid allows for the necessary updating of soil water contents based on changing particle densities and related time-dependent changes in the velocity field. The space domain approach also reflects the fact that spatial concentration patterns and thus travel distances are usually observed in the partially saturated zone. The Euler-Grid is hence necessary to calculate spatial concentration profiles and to properly describe specific interactions between matrix and macropore domain.

2.2 Underlying theory and model equations

2.2.1 Transient fluid flow in the partially saturated zone

The LAST-Model (Sternagel et al., 2019) is based on the Lagrangian approach of Zehe and Jackisch (2016), which was introduced to simulate infiltration and soil water dynamics in the partially saturated zone using a non-linear

5 random walk in the space domain. The results of test simulations (cf. Appendix) confirmed the ability of the Lagrangian approach to simulate water dynamics under well-mixed conditions in different soils, in good accord with simulations using a Richards equation solver. We refer the reader to the study of Zehe and Jackisch (2016) for further details on the model concept.

10 *Derivation of model equations*

The theoretical basis is the soil-moisture form of the Richards equation:

$$\frac{\partial \theta}{\partial t} = \frac{\partial K(\theta)}{\partial z} + \frac{\partial}{\partial z}\left(D(\theta)\frac{\partial \theta}{\partial z}\right), \tag{1}$$

$$\text{with } D(\theta) = K(\theta)\,\frac{\partial \Psi}{\partial \theta}.$$

The K in the first term of Eq. 1 can be initially multiplied by $\frac{\theta}{\theta}$ (= 1) to obtain

$$\frac{\partial \theta}{\partial t} = \frac{\partial}{\partial z}\left[\frac{K(\theta)}{\theta}\,\theta\right] + \frac{\partial}{\partial z}\left(D(\theta)\frac{\partial \theta}{\partial z}\right). \tag{2}$$

20 Re-writing this equation leads to the divergence-based form of the Richards equation:

$$\frac{\partial \theta}{\partial t} = \frac{\partial}{\partial z}\left[\frac{K(\theta)}{\theta}\,\theta - \frac{\partial D(\theta)}{\partial z}\,\theta\right] + \frac{\partial^2}{\partial z^2}\left(D(\theta)\,\theta\right), \tag{3}$$

where z is the vertical position in the soil domain (m), K the hydraulic conductivity (m s^{-1}), D the water diffusivity

25 (m² s[-1]), Ψ the matric potential (m), θ (t) the soil water content (m³ m[-3]) and t the simulation time (s).

Eq. 3 is formally identical to the Fokker-Planck equation (Risken, 1984). The first term of the equation corresponds to a drift/advection term characterizing the advective downward velocity v (m s^{-1}) of fluid fluxes driven by gravity:

$$v(\theta) = \frac{K(\theta)}{\theta} - \frac{\partial D(\theta)}{\partial z}. \tag{4}$$

The second term of Eq. 3 represents diffusive fluxes determined by the soil moisture or matric potential gradient and controlled by diffusivity $D(\theta)$ (cf. Eq. 1). Eq. 3 can then be solved by a non-linear random walk of volumetric water particles (Zehe and Jackisch, 2016). The non-linearity arises due to the dependence of K and D on soil moisture and hence the particle density. The vertical displacement of these particles is described by the Langevin

35 equation:

$$z_i(t + \Delta t) = z_i(t) - \left(\frac{K(\theta_r + i \cdot \Delta \theta)}{\theta(t)} + \frac{\partial D(\theta_r + i \cdot \Delta \theta)}{\partial z}\right) \cdot \Delta t + Z\sqrt{2 \cdot D(\theta_r + i \cdot \Delta \theta) \cdot \Delta t} \qquad i = 1, \dots, N, \tag{5}$$

where the first term describes downward advection of particles driven by gravity on basis of the hydraulic conductivity K (m s⁻¹). The second term describes diffusive transport determined by the soil moisture gradient and controlled by diffusivity $D(\theta)$ (m s⁻¹) in combination with the random walk concept. Here, i is the number of the current bin representing the pore size in which the particle is stored (cf. passage below), and Z a random, uniformly distributed number between [-1, 1].

Model assumptions

The key to simulate soil water dynamics in accord with the Richards equation (in the case of pure matrix flow) and with field observations is to account for the varying mobility of the fluid within different pore sizes. The distribution of particle displacement velocities within the pores is defined by the water diffusivity and hydraulic conductivity curves. These curves are separated into N_B bins (800 bins in the current model version), using a step size of $\Delta\theta = \frac{(\theta(t) - \theta_r)}{N_B}$ from the residual moisture θ_r to the actual moisture $\theta(t)$ (Fig. 1). Based on the actual water content, the water particles are distributed to these bins. This means that particles travel at certain diffusivities and drift velocities corresponding to their bin, which reflects water in different pore sizes. This particle binning concept also enables the simulation of non-equilibrium conditions in the water infiltration process. To that end, a second type of particles (event particles) is introduced to treat infiltrating event water. These particles initially travel at purely gravity-driven velocities in the largest pores and experience a slow diffusive mixing with pre-event particles in the soil matrix during a characteristic mixing time.
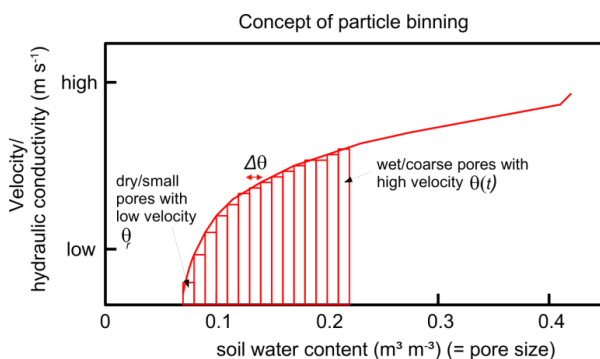
Figure 1. Particle binning concept. All particles within an element of the Euler-Grid are distributed to bins (= red rectangles) representing different pore sizes. Particles travel at various flow velocities and diffusivities depending on their related bin (figure taken from Sternagel et al. (2019)).

2.2.2 Transport of conservative solutes and the macropore domain

Sternagel et al. (2019) extended the LAST-Model with (i) a routine to simulate water and solute transport in soil and (ii) a structural macropore/preferential flow domain. The extended LAST-Model was tested with bromide tracer and macropore data of irrigation experiments at four study sites and compared to simulations of HYDRUS 1-D.

At two sites dominated by well-mixed matrix flow, both models showed equal performance but at two preferential flow dominated sites, LAST performed better (cf. Appendix). We refer to Sternagel et al. (2019) for a more detailed description of the model and results.

5 *Solute transport*

Each water particle is characterized by its position in the soil domain, water mass and a solute concentration. This means that a water particle carries a solute mass that is defined by the product of solute concentration and particle volume. Due to the displacement of a water particle, the dissolved solute masses are transported advectively according to the varying particle displacement velocities. Subsequently to the advective displacement, diffusive

10 mixing of solutes among all water particles in a grid element is calculated by summing their solute masses and dividing this total mass amount by the number of water particles present. Due to this diffusive mixing, the solute mass carried by a water particle may vary in space and time.

Macropore domain

15 LAST offers a structured preferential flow domain consisting of a certain number of macropores that are classified into three depth classes: deep, medium or shallow. The total number of macropores at a study site is distributed over these three depth classes to allow for a depth-dependent mass exchange with the matrix domain. The parameterization of the preferential flow domain and the respective length of each macropore class bases on observable field data, such as the mean numbers of macropores of certain diameters, their hydraulic properties,

20 and length distribution. These structural data can be obtained from field observations or inverse modelling with tracer data, but must not be spatially resolved because LAST operates on the 1-D scale. The actual water content and the flux densities of the topsoil control infiltration and distribution of water particles to both domains. The two processes are further determined by the matric potential gradient and hydraulic conductivity of the soil matrix, together with the friction and gravity within the macropores. After the infiltration, macropores are filled from the

25 bottom to the top by assuming purely advective flow in the macropore domain. Interactions among macropores and matrix are represented by diffusive mixing and exchange of water and solutes between both flow domains, which depends also on the matric potential and water content.

3 Concept and implementation of reactive solute transport into the LAST-Model

The main objective of this study is to present a formulation for reactive solute transport in the LAST-Model, to

30 simulate the movement of reactive substances through the soil zone under the influence of sorption and degradation processes. This is implemented by assigning an additional reactive solute concentration C_{rs} (kg m^{-3}) to each water particle. A water particle hence carries a reactive solute mass m_{rs} (kg), which is equal to the product of reactive solute concentration and its water volume. Transport and diffusive mixing of the reactive solute masses within a time step are simulated in the same way as for the conservative solute (cf. Sect. 2.2.2) (Sternagel et al., 2019).

35 After diffusive mixing, the reactive solute mass of each particle can change due to a non-linear mass transfer (adsorption, desorption) between water particles and the sorption sites of the adsorbing solid phase, which are determined by the substance-specific and site-specific Freundlich Isotherms (cf. Sect. 3.1). The adsorbed reactive solute mass in the soil solid phase can then be reduced by degradation following first-order kinetics driven by the

half-life of the substance (cf. Sect. 3.2). These two reactive solute processes take place in the soil matrix as well as in the wetted parts of the macropores, and their intensity can vary with soil depth as detailed in the following sections. Fig. 2 provides an overview sketch and a flow chart to illustrate sorption and degradation processes and the sequence of reactive solute transport.
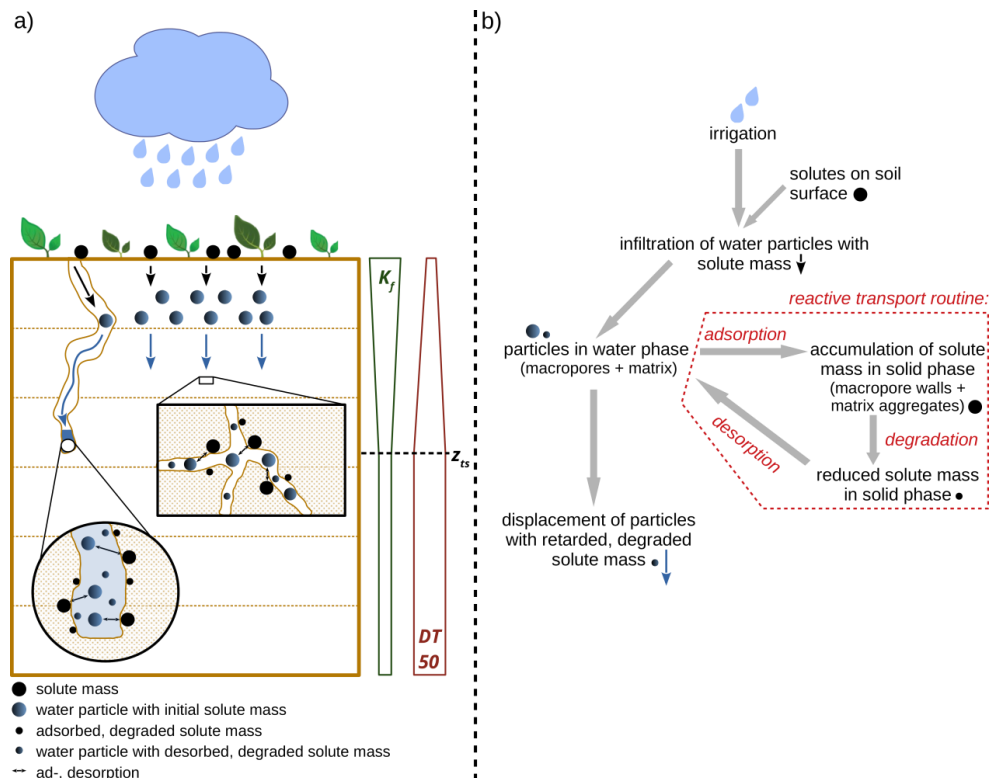
5 **Figure 2. a)** Overview sketch of sorption and degradation processes in the soil domain. Down to the predefined depth z_{ts} (m), we assume the topsoil with linearly-decreasing K_f and linearly-increasing $DT50$ values to account for the depth-dependence of sorption and degradation, respectively. Below z_{ts} in the subsoil, we assume constant values. **b)** Flow chart to illustrate the sequence of reactive solute transport. The pictograms of the sketch are assigned to the respective positions and steps of the flow chart.

10 **3.1 Retardation of solute transport via non-linear sorption between water and solid phase**

3.1.1 Implementation of retardation into the LAST-Model

Retardation and delay of reactive solute transport comprises adsorption and desorption. A commonly applied concept to represent sorption in Eulerian models is to use a retardation coefficient. The retardation coefficient describes how much further a fluid has migrated in a time step compared to a dissolved, sorption-retarded solute.

15 However, this concept is not implementable into the LAST-Model because solute masses are carried by the water particles and hence travel at the same velocity. In LAST, we thus explicitly represent sorption processes by a related transfer of solute masses between the water and soil solid phase. Sorption is described by the partitioning of reactive solute masses between the water particles and the adsorbing phase. The mass balance between both phases is calculated by using the non-linear Freundlich Isotherms of the respective solute and the rate equation

$$m_{rs}(t) = m_{rs}(t - \Delta t) - \left(K_f \, C_{rs}{}^{beta} \right) \left(\frac{m_p}{\rho} \right), \tag{6}$$

where m_{rs} (kg) is the reactive solute mass of a particle, K_f (-) the Freundlich coefficient/constant, C_{rs} (kg m^{-3}) the reactive solute concentration of a particle, $beta$ (-) the Freundlich exponent, m_p (kg) the water mass of a particle,

5   ρ (kg m^{-3}) the water density, t (s) the current simulation time and Δt (s) the time step.

The reversed desorption of adsorbed solutes from the soil solid phase to the water particles is equally calculated by using the solute concentration in the sorbing solid phase, which requires the adsorbed solute mass and the volume of the phase. The sorption process is hence controlled by a macroscopic concentration gradient on the scale of an element of the Euler-Grid between water and solid phase.

10   **3.1.2 Assumptions for the parameterization of the sorption process**

Generally, sorption is a non-linear process, which reflects the limited availability of adsorption sites. This may cause imperfect sorption, which can lead to the observation of early mass arrivals and long tailings in breakthrough curves (e.g. Leistra, 1977). Thus, our approach calculates the non-linear adsorption or desorption of solute masses, as a function of the solute concentration or loading of the sorption surfaces of the sorbent. Hence, in a given time

15   step, the higher the solute concentration in the solid phase, the fewer the solute masses that can be additionally adsorbed from the water phase, and vice versa. In LAST, the sorption processes only proceed until a concentration equilibrium between both phases is reached. At this point, there is no further adsorption or desorption of solute masses until the concentration of one phase is again disequilibrated by, e.g., the infiltration of water into the water phase or by solute degradation in the solid phase. In the case that the concentration of a reactive solute in the water

20   phase is higher than its solubility, the excess solute masses leave solution and are adsorbed to the soil solid phase.

With regard to pesticides, the major pesticide sorbent is soil organic matter and its quantity and quality determines to a large fraction the soil sorption properties (Farenhorst, 2006; Sarkar et al., 2020). Several studies revealed that in the topsoil, enhanced sorption of pesticides occurs due to the often high content of organic matter, which may

25   reflect bioavailability by an increased amount of sorption sites in the non-mineralized organic matter (e.g. Clay and Koskinen, 2003; Jensen et al., 2004; Boivin et al., 2005; Rodríguez-Cruz et al., 2006). This implies that the conditions in the topsoil generally facilitate the sorption of dissolved solutes. While different depth profiles of the K_f value could be implemented depending on available data, to account for this depth-dependence of sorption processes, we here apply a linearly-decreasing distribution of the K_f value over the grid elements of the soil domain

30   between two predefined upper and lower value limits for the topsoil. The depth of the topsoil (z_{ts}) can be adjusted individually and for our applications, we set it to 50 cm. Below this soil depth, we assume the subsoil and apply constant K_f values. The exact K_f parameterizations of the respective model setups at the different sites are explained in Sect. 4.2.1 and 4.2.2, and summarized in Table 2.

35   *Sorption in macropores*

While sorption generally controls pesticide leaching in the soil matrix, the processes are different in macropores. Sorption in macropores is often limited because the time scale of vertical advection is usually much smaller than the time required by solute molecules to diffuse to the macropore walls (Klaus et al., 2014). However, sorption may occur to a significant degree once water is stagnant in the saturated parts of the macropores (Bolduan and

Zehe, 2006). This stagnancy facilitates the possibility for sorption of reactive solutes between macropore water and the macropore walls. The macropore sorption processes are also described and quantified by the Freundlich approach and Eq. 6.

3.2 First-order degradation of adsorbed solutes in soil solid phase

5   **3.2.1 Implementation of degradation into the LAST-Model**

Reactive solutes such as pesticides are commonly biodegraded and therewith transformed into metabolite/child compounds by the metabolism or co-metabolism of microbial communities that are present mainly on the surfaces of soil particles. Sorption processes, and the resulting effects on retarding solute transport, facilitate a time scale for the degradation process, which must be long enough for metabolization but smaller than the time scale for

10   desorption and thus re-mobilization of solutes. Many pesticides are subject to co-metabolic degradation, which often follows first-order kinetics and can hence be characterised by an exponential decay function

$$C_t = C_0\, e^{-k\,t}, \tag{7}$$

15   where C_t (kg m⁻³) is the concentration of the pesticide after the time t (s), C_0 (kg m⁻³) the initial concentration and k (s⁻¹) the degradation rate constant.

Based on the first-order kinetics of Eq. 7, we apply a mass rate equation (Eq. 8) for the degradation of adsorbed solute masses on the macroscopic scale of an element of the Euler-Grid in LAST:

20   $$m_{sp}(t + \Delta t) = m_{sp}(t)\left(1 - \left(k\,\frac{\Delta t}{86400}\right)\right), \tag{8}$$

where $m_{sp}(t)$ and $m_{sp}(t + \Delta t)$ (kg) are the reactive solute masses in the soil solid phase of the current time step and of the next time step after degradation, and Δt (s) the time step. The kinetics of this degradation process are determined by the half-life $DT50$ (d) of the respective substance, with the relationship between $DT50$ and the

25   degradation rate constant k (d⁻¹) given by

$$k = \frac{ln(2)}{DT50}. \tag{9}$$

3.2.2 Assumptions for the parameterization of the degradation process

30   Turnover and degradation of pesticides depend in general on the substance-specific chemical properties and the microbial activity in soils (Holden and Fierer, 2005). Microbial activity in soil depends on many factors, including organic matter content, pH, water content, temperature, redox potential and carbon-nitrogen ratio. As these factors are usually highly heterogeneous in space, considerable research has focused on spatial differences in pesticide turnover potentials. Some of these studies determined that pesticide turnover rates typically decrease within the

35   top meter of the soil matrix (e.g. El-Sebai et al., 2005; Bolduan and Zehe, 2006; Eilers et al., 2012). This is because the topsoil provides conditions that facilitate enhanced microbial activity (Fomsgaard, 1995; Bending et al., 2001; Bending and Rodriguez-Cruz, 2007). Thus, we parameterize degradation as depth-dependent in our model. While

detailed experimental data may allow for a small-scale, heterogeneous description of degradation, this approach can also result in over-parameterization. Thus, we account for the depth-dependence of degradation by applying a simplified, linearly-increasing distribution of the *DT50* value over the grid elements of the soil domain, between two predefined upper and lower limits for the topsoil depth z_{ts}. In the subsoil below 50 cm, we apply constant

5   *DT50* values (cf. Sect. 3.1). In line with the K_f parameter, the exact *DT50* parameterizations of the respective model setups at the different sites are explained in Sect. 4.2.1 and 4.2.2, and summarized in Table 2.

Degradation in macropores

The presence of macropores allow pesticides to bypass the topsoil matrix, while they may infiltrate and thus be

10   more persistent in the deeper subsoil matrix where the turnover potential is decreased. As biopores like worm burrows often constitute the major part of macropores in agricultural soils, a number of studies have focused on their key role for pesticide transformation (e.g. Binet et al., 2006; Liu et al., 2011; Tang et al., 2012). These studies consistently revealed an elevated bacterial abundance and activity in the immediate vicinity of worm burrows (Bundt et al., 2001; Bolduan and Zehe, 2006), comparable to the optimum conditions in topsoil. This is attributed

15   to a positive effect of enhanced organic carbon, nutrient and oxygen supply that may lead to increased adsorption and degradation rates in macropores. Thus, we assume that degradation also takes place in the adsorbing phase of the macropores, which can be quantified with Eq. 8. We apply different K_f and *DT50* values in the macropores that are in the range of the topsoil values (cf. Table 2).

4 Model benchmarking

20   The extended LAST-Model is tested by simulating irrigation experiments using bromide tracer and the herbicide IPU as a representative reactive substance, at two study sites in the Weiherbach catchment (Zehe and Flühler, 2001). These two sites are dominated by either matrix flow under well-mixed conditions (site 5) or preferential macropore flow (site 10) on a time scale of 2 days. These experiments are also simulated with the HYDRUS 1-D model. Further, we use data of a study site (P4) from a field-scale irrigation and leaching experiment (Klaus et al.,

25   2014) in the Weiherbach catchment to test our model on a larger time scale of 7 days. Please note that we refer to these time periods of 2 and 7 days when we discuss, respectively, short-term and long-term time scales in this study.

4.1 Setups of the benchmark experiments

Study area: The Weiherbach catchment

30   The Weiherbach valley extends over a total area of 6.3 km² and is located in the southwest of Germany. The land is used mainly for agriculture. The basic geological formation of the valley is characterized by Pleistocene Loess layer up to 15 m thick, which covers Triassic Muschelkalk marl and Keuper sandstone. At hillfoots, the hillslopes show a typical Loess catena with erosion-derived Colluvic Regosols while at hilltops and -mids, mainly Calcaric Regosols or Luvisols are present. More detailed information on the Weiherbach catchment is provided in Plate

35   and Zehe (2008).

Isoproturon (IPU)

IPU is an herbicide, which is commonly applied in crops to control annual grasses and weeds. IPU has a moderate water solubility of 70.2 mg l^{-1} and is regarded as non-persistent (mean $DT50$ in field: 23 d) and moderately mobile (mean K_f = 2.83) in soils (see also typical K_f and $DT50$ value ranges in Table 2). IPU is ranked as carcinogenic and its turnover in soils forms, mainly, the metabolite desmethylisoproturon (Lewis et al., 2016).

4.1.1 Plot-scale experiments of Zehe and Flühler (2001) at the well-mixed site 5 and the preferential flow dominated site 10

At site 5, the soil moisture and soil properties were initially measured on a defined plot area of 1.4 m x 1.4 m. Before the irrigation, 0.5 g of IPU were applied, distributed evenly, on the surface of the plot area. After one day, the IPU loaded plot area was irrigated by a rainfall event of 10 mm h^{-1} of water for 130 minutes with 0.165 g L^{-1} of bromide. After another day, soil samples were taken along a vertical soil profile of 1 m x 1 m in a grid of 0.1 m x 0.1 m. Thus, ten soil samples were collected in each 10 cm depth interval down to a total depth of 1 m. In subsequent lab analyses, the IPU and bromide concentrations of all samples were measured. The soil at site 5 is a Calcaric Regosol (Working Group WRB, 2014) and flow patterns reveal a dominance of well-mixed matrix flow without considerable influence of macropore flows. This is the reason for using site 5 to evaluate our reactive solute transport approach under well-mixed flow conditions. Table 1 contains all experiment data.

The experiment at site 10 was conducted similarly with the initial application of 1.0 g of IPU on the soil plot and one day later a block rainfall of 11 mm h^{-1} for 138 minutes. The soil at site 10 can be classified as Colluvic Regosol (Working Group WRB, 2014) and shows numerous worm burrows that can facilitate preferential flow. Hence, we select study site 10 for the evaluation of our reactive solute transport approach during preferential flow conditions. The density and depth of the worm burrow systems were examined extensively at this study site. Horizontal layers in different depths of the vertical soil profile were excavated (cf. Zehe and Blöschl, 2004; van Schaik et al., 2014) and in each layer the number of macropores was counted and their diameters and depths were measured. These detailed measurements provided an extensive dataset of the macropore network. Table 1 again contains all experimental data.

4.1.2 Long-term field experiment of Klaus et al. (2014)

Klaus et al. (2014) conducted irrigation experiments in the Weiherbach catchment to investigate, among other aspects, the long-term influence of the connectivity of macropores to tile drains on tracer and pesticide leaching. A series of three irrigation experiments with bromide tracer and IPU were performed on a field site (20 x 20 m) with different small study sites. We focus on the first experiment in which the field site was irrigated in three individual phases with a total precipitation sum of 34 mm over 220 minutes. Additionally, a total of 1600 g of bromide was applied on the field site. We focus on site P4 where soil profiles were excavated and soil samples collected in a 0.1 m x 0.1 m grid down to a depth of 1 m after 7 days, and their corresponding bromide concentrations measured. Patterns of worm burrows in the first 15 cm of the soil were also examined (Table 3). The present soil is a Colluvisol (Working Group WRB, 2014) with a strong gleyic horizon present in a depth between 0.4 and 0.7 m, which causes a decreasing soil hydraulic conductivity gradient with depth that leads to almost stagnant flow conditions in the subsoil (Klaus et al., 2013).

In general, the experiment design, soil sampling and data collection are similar to the experiments of Zehe and Flühler (2001). Initial soil water contents and all further experiment parameters as well as the soil properties at the field site are listed in Table 3.

4.2 Model setups

5   To compare our 1-D simulation results to the observed 2-D concentration data, the latter are averaged laterally in each of the 10 cm depth intervals. Note that the corresponding observations provide solute concentration per dry mass of the soil while the LAST-Model simulates concentrations in the water phase and solute masses in the soil solid phase, respectively. We thus compare simulated and observed solute masses and not concentrations in the respective depths.

10   **4.2.1 Model setups of simulations at well-mixed site 5**

LAST-Model setup at well-mixed site 5

Site 5 is dominated by well-mixed matrix flow. We thus deactivate the macropore domain of LAST and carry out simulations for IPU and bromide at this site. Without the influence of macropores and otherwise moderate hydraulic matrix conditions, we here assume only small penetration depths of solutes through the first top

15   centimetres of the soil, as shown already at other well-mixed sites in the Weiherbach catchment (Sternagel et al., 2019). This means that solutes may remain in the upper part of the topsoil, so that a depth-dependent parameterization of sorption and degradation (cf. Sect. 3.1, 3.2) is (at least in a first step) not necessary at this site. Thus, we apply constant values of K_f and $DT50$ (Table 2) and use mean values under field conditions for IPU from the Pesticide Properties DataBase (PPDB) (Lewis et al., 2016).

20   Consistent with the experiments, we use a matrix discretization of 0.1 m. Initially, the soil domain contains 2 million water particles, but no solute masses. All further experiment and simulation parameters are shown in Table 1.

HYDRUS 1-D setup at well-mixed site 5

25   The simulation with HYDRUS 1-D at the well-mixed site 5 is conducted with a single porosity model (van Genuchten-Mualem) and an equilibrium model for water flow and solute transport, respectively, with the Freundlich approach for sorption and first-order degradation. At the upper domain boundary, we select atmospheric conditions with a surface layer and variable infiltration intensities. At the lower boundary, we assume free drainage conditions. In general, we use the same soil hydraulic properties, model setups, initial conditions and

30   reactive transport parameters as for LAST (cf. Tables 1, 2).

4.2.2 Model setups of simulations at preferential flow dominated site 10

LAST-Model setup for simulations at preferential flow dominated site 10

Based on the extensively observed macropore dataset, we obtain the parameterization of the macropore domain at site 10. The main parameters are thus the depth distribution of the macropore network, mean macropore diameters and the distribution factors (cf. Table 1). The study of Sternagel et al. (2019) explains in detail how the macropore

35   domain of LAST is parameterized based on available field measurements. We vertically discretize the macropores in steps of 0.05 m and assume that they initially contain no water particles and solute masses. A maximum of

10,000 possible particles that can be stored in a single macropore, and hence the total possible number of particles in the entire macropore domain is given by multiplication with the total number of macropores. The studies of Ackermann (1998) and Zehe (1999) provide further descriptions of site 10 and the macropore network.

As the heterogeneous macropore network allows a rapid bypassing of solutes and hence causes a considerable

5 penetration into different soil depths, we use variable values of K_f and $DT50$ for IPU in different soil depths and in the macropores to account for a depth-dependent retardation and degradation (Table 2) for the simulations at site 10. Furthermore, we here use different parameterization setups of the reactive transport routine to account for the remarkably variable value ranges of K_f and $DT50$ found by various studies (e.g. Bolduan and Zehe, 2006; Rodríguez-Cruz et al., 2006; Bending and Rodriguez-Cruz, 2007; Lewis et al., 2016) and hence the wide

10 uncertainty range of the reactive transport behaviour of IPU in the field. Based on the results of these studies, we distinguish between two parameter configurations for a rather weak reactive transport of IPU and a strong reactive transport with enhanced retardation and degradation of IPU (Table 2). To evaluate the impact of the K_f value on the model sensitivity, we furthermore perform a simulation at site 10 only with activated sorption and no degradation. Table 1 contains all relevant simulation and experiment parameters.

HYDRUS 1-D setup at preferential flow dominated site 10

The simulation with HYDRUS 1-D at the preferential flow dominated site 10 are performed with the same model setups, soil properties, initial and boundary conditions as well as reactive transport parameters as for the simulations with LAST (cf. Tables 1, 2). In contrast, we select a dual-permeability approach for water flow ("Gerke

20 and van Genuchten, 1993") and solute transport ("Physical Nonequilibrium") at this site. These approaches distinguish between matrix and fracture domains for water flow and solute transport. It applies the Richards equation for water flow in each domain, with domain-specific hydraulic properties. The advection-dispersion equation is used to simulate solute transport and mass transfer between both domains, including terms for reactive transport with retardation and degradation (Gerke and van Genuchten, 1993). While we apply the same soil

25 hydraulic properties in the matrix (cf. Table 1) as for the LAST simulations, the macropore domain in HYDRUS gets a faster character with a K_s value of 10^{-3} m s^{-1}. We also select the Freundlich approach for sorption processes and first-order degradation.

4.2.3 LAST-Model setup of long-term simulations at site P4

We perform simulations for conservative bromide tracer and reactive IPU at site P4 on a time scale of 7 days.

30 Based on examination of the macropore network, we again derive the parameterization of the macropore domain (Table 3). In line with the LAST-Model setups in Sect. 4.2.1 and 4.2.2, we apply the same discretization of the matrix (0.1 m) and macropore (0.05 m) domain as well as the number of particles in both domains (2 million; 10 k per macropore grid element). Initially, macropores and matrix contain no solute masses, and the macropores also contain no water.

35 For the simulation of reactive IPU transport, we again apply the weak and strong reactive transport parameterizations with the depth-dependent K_f and $DT50$ values of the simulations at site 10 (cf. Table 2). An evaluation with observed IPU mass profiles is not possible here because robust experimental data are missing. All relevant parameters of the long-term simulations at P4 are listed in Table 3.

Table 1. Parameters of IPU experiments and simulations, and soil hydraulic parameters, at sites 5 and 10. Where K_s is the saturated hydraulic conductivity, θ_s the saturated soil water content, θ_r the residual soil water content, α the inverse of an air entry value, n a quantity characterizing pore size distribution, s the storage coefficient and ρ_b the bulk density. Further, *mac. big*, *mac. med* and *mac. sml* describe the lengths of big, medium and small macropores as well as f_{big}, f_{med} and f_{sml} are the respective distribution factors to split the total number of macropores to these three macropore depths. For further details on these parameters, please see Sternagel et al. (2019).

Parameter	Site 5	Site 10
Irrigation duration (hh:mm)	02:10	02:18
Irrigation intensity (mm h⁻¹)	10.70	11.00
Applied IPU mass (kg)	$5 \cdot 10^{-4}$	$1 \cdot 10^{-3}$
Recovery rate (%)	84.4	91
Initial soil moisture in 15 cm (%)	23.7	27.8
Simulation time t (s)	172,800 (= 2 Days)	
Time step Δt (s)	dynamic	
Particle number in matrix (-)	2 Mill.	
Particle number in macropore domain (-)	-	920 k
Soil type	Calcaric Regosol	Colluvic Regosol
K_s *(m s⁻¹)*	$1.00 \cdot 10^{-6}$	$1.00 \cdot 10^{-6}$
θ_s *(m³ m⁻³)*	0.46	0.46
θ_r *(m³ m⁻³)*	0.04	0.04
α *(m⁻¹)*	4.0	3.0
n *(-)*	1.26	1.25
s *(-)*	0.38	0.38
ρ_b *(kg m⁻³)*	1300	1500
Number of macropores (-)	-	92
Mean macropore diameter (m)	-	0.005
mac. big (m)	-	0.8
mac. med (m)	-	0.5
mac. sml (m)	-	0.2
f_{big} *(-)*	-	0.14
f_{med} *(-)*	-	0.37
f_{sml} *(-)*	-	0.49

Table 2. Reactive transport parameters at the sites 5 and 10. The upper and lower value limits in the squared brackets describe the value ranges of the depth-dependent K_f and *DT50* parameters between soil surface and the starting depth of the subsoil (cf. Fig. 2, Sect. 3.1.2, 3.2.2). At site 10, we distinguish between two parameter configurations for a rather weak reactive transport of IPU and a strong reactive transport with enhanced retardation and degradation of IPU.

Parameter	Site 5	Site 10 weak configuration	Site 10 strong configuration
K_f *for IPU in soil matrix (-)* *[upper limit; lower limit]*	[2.83; 2.83]	[1; 0.26]	[27; 3]
DT50 for IPU in soil matrix (d) *[upper limit; lower limit]*	[23; 23]	[23; 44]	[3; 12]
K_f *for IPU in macropores (-)*	-	5	10
DT50 for IPU in macropores (d)	-	15.6	10
beta (-)	0.8	0.8	0.8

Table 3. Parameters of long-term bromide experiments and simulations as well as soil hydraulic parameters at site P4 (Klaus et al., 2014). For parameter definitions and further details on these parameters, see Table 1 and Sternagel et al. (2019). Note that only one macropore depth of 15 cm was observed at this site.

Parameter	P4
Irrigation duration (hh:mm)	03:40

Total irrigation sum (mm)	34.00
Applied bromide mass on field site (kg)	1.6
Recovery rate (%)	~ 100
Initial soil moisture in 10 cm (%)	24.8
Initial soil moisture in 20 cm (%)	27.1
Initial soil moisture in 30 cm (%)	27.0
Initial soil moisture in 40 cm (%)	28.44
Initial soil moisture in 60 cm (%)	33.11
Initial soil moisture in 100 cm (%)	29.60
Simulation time t (s)	604,800 (= 7 days)
Time step Δt (s)	dynamic
Particle number in matrix (-)	2 Mill.
Particle number in macropore domain (-)	680 k
Soil type	Colluvisol
K_s in: topsoil; gleyic horizon (subsoil) (m s^{-1})	$1.00 \cdot 10^{-5}$; $1.00 \cdot 10^{-8}$
θ_s in: topsoil; gleyic horizon (subsoil) (m³ m^{-3})	0.50; 0.4
θ_r in: topsoil; gleyic horizon (subsoil) (m³ m^{-3})	0.04; 0.11
α in: topsoil; gleyic horizon (subsoil) (m^{-1})	1.9; 3.8
n in: topsoil; gleyic horizon (subsoil) (-)	1.25; 1.20
s (-)	0.38
ρ_b (kg m^{-3})	1500
Number of macropores (-)	68
Mean macropore diameter (m)	0.003
mac. big (m)	0.15
mac. med (m)	-
mac. sml (m)	-
f_{big} (-)	1.0
f_{med} (-)	-
f_{sml} (-)	-

5 Results

In the following sections, we present simulated mass profiles of bromide and IPU at the different study sites (cf.
5   Sect. 4.1). The profiles result from model runs with different parameter setups and time scales (cf. Sect. 4.2). We compare LAST simulation results with those of HYDRUS 1-D. Note that all presented IPU mass profiles represent total masses in each soil depth, i.e. the sum of IPU masses in the water and soil solid phase.

5.1 Simulation results at the well-mixed site 5

5.1.1 IPU transport simulated with LAST

10   In general, the three simulated IPU profiles in Fig. 3a indicate significant retardation and degradation, with remarkable differences between the profiles already after 2 days, due to the non-persistent character of IPU and the commonly short lag-phase in topsoils (cf. Sect. 6.1.1).

The reference simulation treating IPU as conservative (red profile) overestimates the transport of IPU into soil depths lower than 10 cm, with a maximum penetration depth of 40 cm, which in turn leads to simultaneous
15   underestimation of masses in the shallow, surface-near soil depths (RMSE: 0.064 g, 12.8 % of applied mass). In

the case of the simulation with retardation and no degradation (yellow profile), the simulated mass profile matches the observed profile in the first 10 cm, because retardation causes mass accumulation. With additional degradation (light blue profile), the solute masses in the first 10 cm are then slightly reduced due to the moderate *DT50* value of 23 days and the relatively short simulation period of 2 days. Overall, the simulation with retardation and

5   degradation is in better accord with the observed mass profile, which is reflected by a smaller RMSE value of 0.027 g (5.5 % of applied mass). At the end of the simulated period of two days, a total IPU mass of 0.014 g is degraded while the observed profile has a mass deficit of 0.078 g. This observed deficit with a recovery rate of 84 % in the experiment may hence be due not only to degradation, but also by mass losses in the experiment execution and lab analyses; in contrast, our model is mass conservative.

10   **5.1.2 IPU transport simulated with HYDRUS 1-D**

The IPU mass profile simulated with HYDRUS 1-D (Fig. 3b), with activated reactive transport, show similar mass patterns compared to LAST and the observed profile with a RMSE value of 0.036 g (7.3 % of applied mass). While HYDRUS overestimates the IPU masses at the soil surface, considering a stronger retardation compared to the observation and the LAST results, it simulates the observed masses in 10-20 cm soil depth quite well. In these

15   depths, LAST overestimates masses with a maximum penetration depth of 30 cm, which is 10 cm deeper than observed. Overall, the results of HYDRUS are consistent with both the LAST and observed profile. HYDRUS simulates a total, degraded IPU mass of 0.017 g, which is in range with the LAST results (cf. Sect. 5.1.1). This means that in both models, the total degradation is similar but the distribution of the remaining IPU masses over the soil profile differs.

20   **5.1.3 Bromide transport simulated with LAST**

Bromide slightly percolates into greater depths during the short-term irrigation experiment (Fig. 3c) compared to the retarded and degraded IPU (cf. Fig. 3a). The results generally underline that LAST is able to simulate conservative solute transport under well-mixed conditions, as we have already shown in our previous study (Sternagel et al., 2019) (cf. Appendix). The results further show that LAST is capable of treating both conservative

25   tracers and reactive substances.
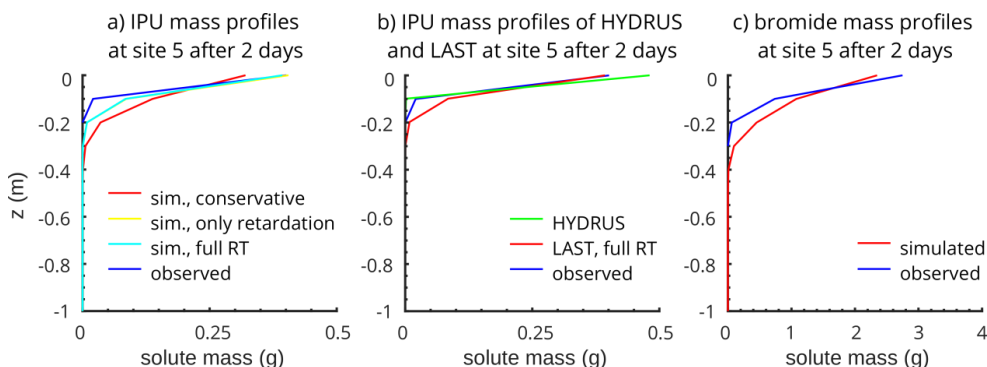
Figure 3. a) LAST-Model results of reactive IPU transport simulations at the well-mixed site 5 after 2 days with regarding IPU as conservative without reactive transport which serves as reference (red profile), with activated retardation but without degradation to exclusively show the effect of the sorption processes (yellow profile) and with fully activated reactive transport

(light blue profile). **b)** Comparison with HYDRUS 1-D results and **c)** exemplary results of a conservative simulation with LAST for bromide.

5.2 Simulation results at the preferential flow dominated site 10

5.2.1 IPU transport simulated with LAST

5   Fig. 4a and 4b present results of different simulation setups compared to the observed IPU mass profile at site 10 after 2 days. Both figures comprise the observed profile as well as a profile of a reference simulation treating IPU as conservative. Fig. 4a focuses on the mass profiles resulting from simulations only with activated retardation, using low and high K_f values. Fig. 4b shows results for simulations performed with full reactive transport subject to retardation and degradation, using parameterizations for weak and strong reactive transport. The shaded area

10   between these profiles represent the uncertainty ranges of simulated transport corresponding to the variations of the empirical K_f and $DT50$ values (cf. Table 2).

In general, the typical "fingerprint" of preferential flow through macropores is clearly visible in the observed IPU mass profile. The observed mass accumulations and peaks fit well to the observed macropore depth distribution (cf. Table 1), which implies that water and IPU travelled through the macropores and infiltrated into the matrix in

15   the respective soil depths where the macropores end. The observed mass profile shows a strong accumulation of IPU masses in depths between 70-90 cm, which cannot be explained by the relatively low number of macropores (~ 13) in this depth. One reason for this could be particle-bound transport of IPU at this study site, as proposed by Zehe and Flühler (2001). In comparison, the simulated conservative reference profile depicts the observed mass distribution quite well on average, although less well the heterogeneous profile shape with a RMSE value of 0.076

20   g (7.6 % of applied mass). The mass peaks in the depths of the macropore ends (cf. Table 1) are relatively weak, because solute masses leaving the macropores are not retarded in the matrix but instead flushed out by the water flow into deeper soil depths, resulting in a smoothed mass profile. In the surface-near soil depths between 0-10 cm, the conservative reference simulation clearly overestimates the IPU masses.

The resulting range of reactive solute transport simulations, between the profiles for a weak and strong reactive

25   transport (Fig. 4b), matches the observed profile in terms of both mass amounts and shape, with a RMSE value of 0.038 g (3.8 % of applied mass). Hence, at this site, LAST performs better with activated reactive transport compared to the conservative reference setup. At the matrix depths where the macropores end, there are clear mass accumulations detectable as solutes are adsorbed and retarded after they infiltrated the soil matrix from the macropores. While the simulation with full reactive transport also overestimates the IPU masses in the upper 10

30   cm, the simulated and observed mass profiles coincide well in the lower depths. The observed mass peak at 70-90 cm cannot be reproduced completely. Furthermore, the wider ranges between the simulated profiles for weak and strong reactive transport in the topsoil underpin the influence of the depth-dependent parameterization of especially the $DT50$ values. The higher IPU amounts and lower $DT50$ values in the topsoil lead to higher total degradation in the first centimetres of the soil compared to greater soil depths. In deeper soil layers, degradation is decreased and

35   no difference between the weak and strong reactive transport parameterizations is visible, due to smaller IPU amounts and the constant and rather non-reactive parameterization in the subsoil. The total degraded IPU masses are between 0.026 g and 0.131 g for the weak and strong reactive transport simulations, respectively. The relatively high observed IPU mass recovery of 0.908 g (~ 91 %) implies a possible degraded total mass of 0.092 g, which is consistent with our simulated range.

The simulation only with retardation, in Fig. 4a, reveal hardly any differences between the profiles simulated with high and low K_f values. This implies that the amounts of adsorbed masses are almost equal for different K_f values at the end of the simulation, and thus independent of the K_f value. This might be due to non-linear adsorption, which establishes an equilibrium state between water and the adsorbing phase after a certain time (cf. Sect. 3.1).

5 Hence, independent of the magnitude of K_f, no further adsorption occurs unless degradation is activated, which would lead to mass loss in the soil solid phase and a renewed adsorption potential (cf. Fig. 4b). Higher K_f values lead only to a shorter time to reach this equilibrium state; the final adsorbed masses are similar for different K_f values due to the inactivated degradation in this special case.

5.2.2 IPU transport simulated with HYDRUS 1-D

10 In contrast to the simulations at site 5, IPU mass profiles simulated with the dual-permeability approach of HYDRUS 1-D (Fig. 4c) do not match the heterogeneous shape of the observed profile at site 10 with the mass accumulations in the depths of the macropore ends (cf. Table 1), resulting in a RMSE value of 0.079 g (7.9 % of applied mass). In the first 35 cm, HYDRUS simulates a strong retardation and overestimation of masses with a maximum penetration depth of only 50 cm. In comparison, the LAST-Model performs better at this site (cf. Sect.

15 5.2.1) but again, the total degraded IPU masses of 0.028 g and 0.183 g for the weak and strong reactive transport parameterizations simulated with HYDRUS are similar to the degraded masses resulting from our LAST-Model.
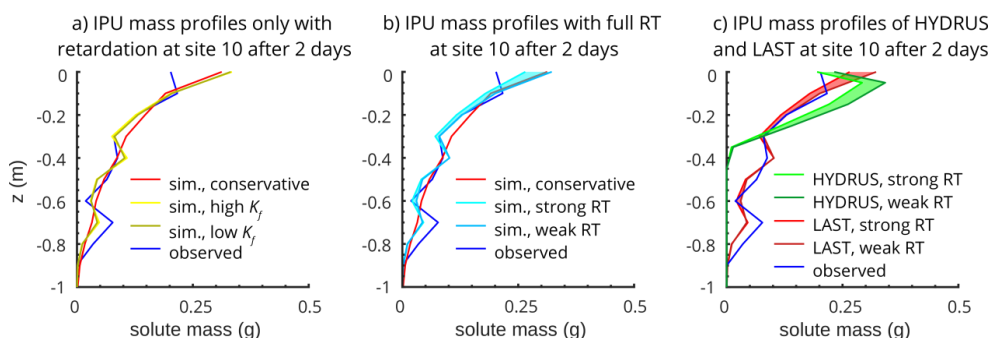
Figure 4. LAST-Model results of reactive IPU transport simulations at the preferential flow dominated site 10 after 2 days. **a)**
20 The simulation is performed only with active retardation and with low and high values for K_f. **b)** The simulation is performed with activated retardation and degradation. The shaded area between the profiles with weak and strong reactive transport (cf. Table 2) shows the uncertainty area of the empirical K_f and $DT50$ values. **c)** Comparison with HYDRUS 1-D simulation results.

5.3 Long-term simulation results at site P4

5.3.1 Long-term bromide transport simulated with LAST

25 Fig. 5a shows the results of the long-term simulation with the simulated and observed bromide mass profiles at site P4 after 7 days. Comparisons of simulated and observed masses directly at the surface are not meaningful because in the experiments, the soil sampling just started in a depth of 5 cm. Additionally, we adjust the input masses in our model in the way that the simulated and observed recovery mass of 6.3 g are equal at the end. This enables a robust comparison of how the same amount of bromide masses distribute over the soil profile in the

30 experiment and simulation.

In the observed profile, there are generally two distinct mass peaks. One peak, at 15-30 cm, probably originates from solute masses leaving the macropores and entering the matrix in 15 cm depth, and subsequently being displaced by water movement into this depth range within the 7 days. The second mass accumulation in a depth around 60-70 cm can be explained by the less permeable gleyic horizon at this soil depth, which leads to ponding

5 of water and solutes. In comparison, the simulated bromide mass profile is generally shifted to greater depths, although the shape corresponds quite well to the observed profile. In the 5-30 cm depth, the simulated masses are underestimated, and conversely, they are overestimated in the following 30-55 cm depth. Obviously, LAST simulates solute displacement that is too strong and fast into these deeper soil depths ("deep shift"), compared to the observed mass accumulation (15-30 cm), after solute masses leave the macropores and enter the matrix in 15

10 cm depth. The simulated mass accumulation in the gley horizon coincides quite well with the observed data, but with long tailing. Despite the almost stagnant conditions in the gley horizon, LAST simulates too strong a displacement of solutes into soil depths even deeper than 1 m (Fig. 5a).

5.3.2 Long-term IPU transport simulated with LAST

Fig. 5b shows the results of a long-term simulation with 6.3 g of IPU applied to the surface. It is thus a kind of

15 extrapolation to give insights of how IPU mass profiles might have temporally evolved at this site for different reactive transport parameterizations, because comparable observed data are unavailable (cf. Sect. 4.2.3, Table 2). The depth transport of IPU is limited compared to bromide because it is retarded and degraded in the topsoil. However, there are again two clear mass peaks along the 15 cm deep macropores and in the depth of the gley horizon. In the topsoil, the differences between the two profiles of a weak and strong reactive transport

20 parameterization are the greatest because, especially in these shallow soil depths, the retardation and degradation rates as well as the amount of IPU are enhanced. The general decreased potential for sorption and degradation processes in the subsoil leads to negligible differences between the profiles in greater soil depths. In total, the degraded IPU masses for the two parameterizations lie between 0.514 g and 2.618 g.
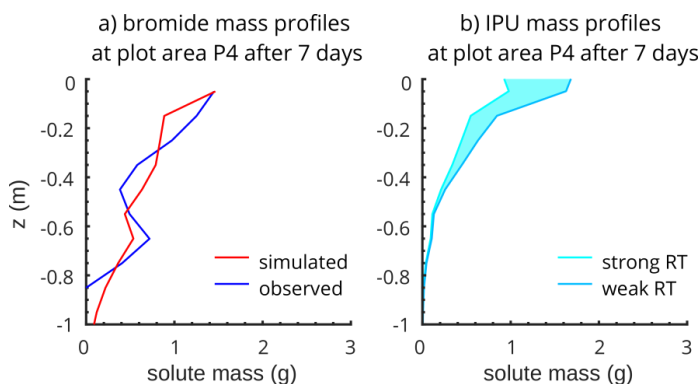
25 **Figure 5. a)** LAST-Model results of long-term simulation with bromide at the site P4 after 7 days. **b)** Shows hypothetical results of a long-term simulation with again a weak and strong reactive transport configuration for IPU (cf. Table 2, Sect. 4.2.3) at the site P4. The bright blue range between the two profiles demonstrates a hypothetical and possible range of IPU mass profiles under the influence of retardation and degradation during 7 days at this site.

6 Discussion

The key innovation of this study is an approach to simulate reactive solute transport in the vadose zone within a Lagrangian framework. We therefore extend the LAST-Model (Sternagel et al., 2019) with a reactive solute transport routine to account for sorption and degradation processes, based on Freundlich Isotherms and first-order

5   decay, during transport of reactive substances such as pesticides through a partially saturated soil domain. The model evaluation with data from irrigation experiments, that examined leaching of bromide and IPU under different flow conditions, shows the suitability of the approach and its physically valid implementation. Comparison to results of HYDRUS 1-D corroborates this finding.

However, in the entire context of this study, it should be recognized that the mean values of K_f and $DT50$ at site 5

10   (cf. Table 2, Sect. 4.2.1) from the PPDB Database were determined empirically at other field sites. Measurements of these variables are laborious and not straightforward, as controls on sorption and degradation vary in space and time (Dechesne et al., 2014). The use of literature values for these parameters introduces considerable uncertainty into pesticide fate modelling (Dubus et al., 2003). As discussed in Sect. 6.1.2, we account for this uncertainty by varying the K_f and $DT50$ values at site 10 in the ranges provided by the PPDB Database and further literature (cf.

15   Table 2, Sect. 4.2.2). We discuss model sensitivities that are, at least for $DT50$, comparable to those found by Sternagel et al. (2019) for simulated tracer transport in a macroporous soil subject to variations in the saturated hydraulic conductivity K_s (cf. section 6.1.3). Further, as discussed in Sect. 6.2, the one-week simulations shed light on the fate of tracers and pesticides in the subsurface on a larger time scale as well as hint at a possible problem of artificial over-mixing of solutes in the gridded soil domain.

20   **6.1 Sorption and degradation in the Lagrangian framework**

6.1.1 Reactive transport under well-mixed conditions

The short-term (2 days) simulations of IPU transport at the well-mixed site 5 corroborate the validity of the underlying assumptions and the way in which degradation and particularly sorption processes are implemented into the Lagrangian framework of the LAST-Model (Fig. 3a). Adsorption causes an expected accumulation of IPU

25   in topsoil layers (0-10 cm) and, consequently, reduced percolation into greater soil depths. Although degradation has only a small impact at this short time scale, due to the moderate $DT50$ value of 23 days, we nevertheless observe a total degradation of 0.014 g IPU in two days that occurs especially in the shallow soil areas where IPU accumulates. The mass profile simulated with retardation and degradation is more consistent with the observations than the reference simulation treating IPU as a conservative solute. Such fast reaction and degradation of IPU in

30   the topsoil can be explained by its general non-persistent and moderately mobile character, as well as an obviously very short duration of a lag-phase near the soil surface which was also discovered by several field studies (e.g. Bending et al., 2001; Bending et al., 2003; Rodríguez-Cruz et al., 2006). The simulated mass profiles of the benchmark simulations with the commonly used HYDRUS 1-D model are also in accord with the observations and corroborate our results; in particular, the total degraded masses are in a similar range (Fig. 3c, Sect. 5.1). This

35   suggests that the developed reactive transport routine of the LAST-Model performs similarly to that implemented in HYDRUS 1-D at this well-mixed site 5. This finding is in line with our previous study, which revealed that both models yielded similar simulations of conservative tracer transport at matrix flow dominated sites (cf. Sternagel et al., 2019).

6.1.2 Impact of the macropore domain on reactive transport under preferential flow conditions

The simulation results at the preferential flow dominated site 10 show that (i) the Lagrangian approach is capable of reproducing the observed heterogeneous IPU mass profile, and (ii) the implemented depth-dependent sorption and degradation processes are particularly helpful in this context (cf. Fig. 4). These results corroborate the importance of the structural representation of macropores in the LAST-Model, consistent with the results of Sternagel et al. (2019). This is also reflected by the fact that the simulated IPU masses in the topsoil between 10-30 cm, and particularly the mass accumulations at the depths where macropores end (cf. Table 1), match the observations, compared to the reference simulation treating IPU as conservative tracer and to simulations with HYDRUS 1-D. Thus, explicit representation of the macropore system with its connectivity, diameter and depth distribution, and treatment of macropore flow and exchange with the matrix, is a feasible approach to reproduce solute bypassing of the topsoil matrix and subsequent infiltration into the subsoil matrix.

HYDRUS 1-D does not match the heterogeneous shape of the observed mass profile at site 10, despite the use of a dual-permeability approach and the same parameterization as LAST. HYDRUS 1-D barely accounts for IPU bypassing and breakthrough to greater depths, and it overestimates retardation in topsoil, which results in a high mass accumulation in the first 10 cm of soil. The total degraded IPU masses are similar in both models, and in accord with the observed data, as both models rely on first-order degradation (Gerke and van Genuchten, 1993). These results hence corroborate the findings of Sternagel et al. (2019), who concluded that HYDRUS is effective under well-mixed conditions but is limited in terms of simulating preferential flow and partial mixing between matrix and macropore flow regimes (e.g. Beven and Germann, 1982; Šimůnek et al., 2003; Beven and Germann, 2013; Sternagel et al., 2019). We propose that incorporating a similarly structured macropore domain into HYDRUS would likely improve simulations under such conditions.

However, all simulated IPU mass profiles at site 10 overestimate the observed masses within the upper 10 cm of the soil. This may be due to an additional photochemical degradation at the soil surface, surface losses due to volatilization, or even plant uptake (Fomsgaard, 1995). Such processes are difficult to detect and parameterize. A possible reason for the mismatch of the observed and simulated mass profiles in 70 cm soil depth at site 10 could be a facilitated pesticide displacement due to particle-bound transport (Villholth et al., 2000; de Jonge et al., 2004). Zehe and Flühler (2001) suggested that IPU is adsorbed to mobile soil particles or colloids at the soil surface, which then travel rapidly through macropores into greater depths at this site.

6.1.3 Sensitivity to variations of sorption and degradation parameters

The ranges of the K_f and $DT50$ values for the case of a weak and strong reactive transport parameterization cause differences in the resulting mass profiles (cf. shaded areas in Fig. 4). These differences are generally stronger in topsoil and gradually decrease with depth. This is because (i) sorption and degradation rates are, due to the higher IPU masses, larger in topsoil than in the subsoil, and (ii) due to the depth-dependent parameterization (cf. Sect. 3). The results of the simulation with only sorption, and no degradation (Fig. 4a), suggest a moderate to low model sensitivity to the K_f parameter. This may be due to the establishment of an equilibrium state between water and soil solid phase during the simulation time of 2 days. In LAST, the amount of adsorbed masses depend mainly on the substance concentration in water and the soil solid phase. As long as the solute concentration in the water phase is higher than in the solid phase, solutes are adsorbed until an equilibrium concentration between both phases is achieved (cf. Sect. 3.1). This means that sorption is also dependent on factors that can disturb this equilibrium

state, to enable further sorption. One such factor could be solute mass loss in the soil solid phase due to degradation, which, if not accounted for as in this special case, leads to a stable equilibrium state once it is achieved. Thus, at the end of the simulations with different parameterizations, the amount of solute masses and their distribution are almost always equal, independent of the K_f value. The magnitude of the K_f value alone only determines how fast

5   the equilibrium state arises. For the simulation with small K_f values, an equilibrium state in all soil depths is reached approximately 1 day after pesticide application, while only about 144 minutes are required for the simulation with the high K_f values.

As for the simulation with both retardation and degradation (Fig. 4b), degradation is also dependent on sorption and the K_f value because degradation only takes place in our approach as long as solute masses are being adsorbed,

10   and hence solutes are present in the soil solid phase. This shows the general mutual dependence of sorption and degradation processes.

6.2 Insights from the long-term simulations and indicators for over-mixing

We first perform a long-term (7 days, cf. Sect. 4) simulation with bromide as a conservative tracer; this is suitable particularly to investigate possible over-mixing (cf. Sect. 1), because no mass is lost due to degradation. Despite a

15   reasonably good match of the observed bromide mass profile (Fig. 5a), we indeed find indications that over-mixing could occur in LAST over longer time scales (cf. Sect. 5.3). While the described "deep shift" and accumulation of bromide masses in soil depths between 30-55 cm (cf. Sect. 5.3.1) could reflect the uncertainty of soil hydraulic properties like the saturated hydraulic conductivity K_s, the long mass tail underneath the mass accumulation in the gleyic subsoil around 70 cm depth probably results from artificial over-mixing. Note that the low-permeable gley

20   horizon in this depth has a K_s value of the order of 10^{-8} m s^{-1}, which implies highly stagnant conditions and thus strongly reduced advective particle movement. Nevertheless, particle diffusion (driven by the random walk, Eq. 5) still occurs due to the particle density and thus water content gradient in this depth originating from the particle accumulation above the gley horizon. Particle diffusion entails diffusive transport of solute masses into deeper soil depths. However, this mass transport might be too strong in our model, as the perfect mixing of solute masses

25   between all water particles in a grid element (Sternagel et al., 2019), leads to small, systematic errors in each time step. These errors accumulate on the long-term scale and result in over-predictions of the displaced solute masses transported by the diffusing water particles (Green et al., 2002). In particular, the subsequent infiltration of pure water particles with zero solute concentration has the potential to "flush out" solutes, leading to the clear tailing of bromide masses even deeper than 1 m (Fig. 5a).

30   We argue that in natural soils, solutes spread diffusively across water stored in different pore sizes (Kutílek and Nielsen, 1994). Hence, diffusive mixing into and out of these pores, as well as their entrapment, depend strongly on the pore size. This implies a time scale for diffusive mixing between the pore sizes and a flushing-out process that is significantly larger than assumed in our perfectly-mixed approach.

The results of the second long-term simulation with exactly the same model setup but with activated reactive

35   transport for IPU does not show any indication for over-mixing (Fig. 5b). This is probably due to the retardation and degradation processes that hinder, or mask, a possible over-mixing as solute masses are adsorbed to the soil solid phase and degraded. Based on the previous findings, we can only assume that the resulting long-term IPU mass profiles are also "deep shifted" due to over-mixing; but comparable data are required for analysis.

6.3 General reflections on Lagrangian models for solute transport

In line with other Lagrangian models using particle tracking for solute transport (e.g. Delay and Bodin, 2001; Berkowitz et al., 2006), our approach shares common assumptions and characteristics. Either particles represent solutes or as in LAST, water parcels, which carry solute masses through the soil domain; and simultaneously, the particles are not independent but interact with each other as well as with the soil domain by sorption and degradation.

However, LAST has important differences compared to some other new particle-based models (e.g. Engdahl et al., 2017; Engdahl et al., 2019; Schmidt et al., 2019), which have been published recently as an alternative to the common solute transport approaches discussed in the introduction. These models do not use a spatial discretization of the soil domain to describe mass transfer between water and soil solid phase. Instead, they use a co-location probability approach, which describes solute particle interactions like mass transfer based on a reaction probability dependent on the distance between a pair of particles. This approach has advantages in simulating transport and reactions of multiple substances on larger spatial scales of geochemical systems like aquifers, compared to the use of an Euler-Grid. It also offers advantages to overcome the described artificial over-mixing problem of Eulerian control volumes (cf. Sect. 1, 6.2). However, this approach also has drawbacks. For example, the miRPT algorithm of Schmidt et al. (2019) transfers all solute masses from mobile particles (= water phase) to immobile particles (= soil solid phase) for reaction and subsequently back to the mobile particles for further transport. Solute reactions like degradation are calculated only for the immobile particles. Therefore, all eligible solute masses must be necessarily transferred to those immobile particles at first, which implies that a sufficient spatial distribution and a large number of immobile particles is necessary. Due to the usage of a spatially discretized soil domain, LAST is in contrast able to perform specific reaction calculations for the partial mass transfer between water and soil solid phase. This is more efficient for transport simulations at the 1-D plot scale, and is less time-consuming and computationally intensive than the approach of the miRPT algorithm. Furthermore, these Lagrangian particle-tracking approaches ultimately require a spatial discretization to calculate solute concentrations, which they achieve by grouping of adjacent particles within a specifically defined radius. This approach is thus similar to soil domain discretization of Eulerian methods, which justifies the Euler-Grid in LAST.

In general, the extended LAST-Model with an accounting for reactive solute transport requires only a moderate increase in simulation times compared to the originally published model version (Sternagel et al., 2019). A total simulation time of only 20 to 30 minutes on a moderately powerful PC is required for simulations at the heterogeneous site 10 over 2 days, which we consider reasonable relative to the improved model functionality and physical soundness.

7 Conclusions and Outlook

Overall, the main findings of this study are that:

- Simulation results demonstrate the feasibility of the approach to simulate reactive transport in a Lagrangian model framework (cf. Sect. 6.1.1).
- Comparisons to results of HYDRUS 1-D underline that the structural macropore domain is an asset of LAST, which enables an accounting of preferential bypassing and re-infiltration of solutes (cf. Sect. 6.1.2).

- LAST shares common assumptions with other alternative particle-based models but has beneficial characteristics for the simulation of reactive solute transport in partially saturated soil plots (cf. Sect. 6.3).
- Long-term simulations show that, while the current formulation yields reasonably good results for bromide transport, some over-mixing of solutes via diffusion is present (cf. Sect. 6.2).

In future work, we intend to address the over-mixing phenomenon and possible improvements to the LAST formulation, to better quantify solute transport over longer time scales. One option would be to perform long-term soil column experiments to examine how tracers and pesticides diffusively enter and leave different pore sizes. Based on such experiment results, one could improve the solute transport routine to better account for mixing

10 between water particles that are stored in pores of different size. The LAST-Model offers promising opportunities in this regard, as it distinguishes particle movements in different velocity bins, which represent water in different pore sizes (cf. Sect. 2). In this way, it may be possible to simulate, in each time step and grid element, the solute mass exchange between water particles using a specific diffusive transfer rate that is dependent on the pore size or bin in which the particles are stored. With this approach, we would overcome the perfect mixing assumption and

15 may apply pore size-specific sorption with a bin-dependent gradient of K_f values.

Data availability. The previously published version of the LAST-Model (Sternagel et al., 2019) is already available in a GitHub repository: https://github.com/KIT-HYD/last-model (Mälicke and Sternagel, 2020). We also intend to provide the extended model version of this study with reference data and the presented test experiments in this

20 repository. Otherwise, please contact Alexander Sternagel (alexander.sternagel@kit.edu).

Author contributions. AS wrote the paper, did the main code developments and carried out the analysis. JK and EZ provided the data. RL, JK, BB and EZ contributed to the theoretical framework and helped with interpreting and editing.

Competing interests. The authors declare that they have no conflict of interest.

Financial support. The article processing charges for this open-access publication were covered by a Research Centre of the Helmholtz Association.

Appendix: Previous results of Zehe and Jackisch (2016) and Sternagel et al. (2019)

The following two figures are exemplary results from the previous studies of Zehe and Jackisch (2016) and Sternagel et al. (2019). They generally demonstrate that the Lagrangian approach with its binning concept is able

5 to simulate well equilibrium water dynamics in accord with solutions using a Richards equation solver, and that the approach is superior compared to a naive random walk approach (Fig. A1). Furthermore, Fig. A2 shows the ability of the extended LAST-Model to depict observed tracer mass profiles even under preferential flow conditions, and more effectively than solutions using HYDRUS 1-D.
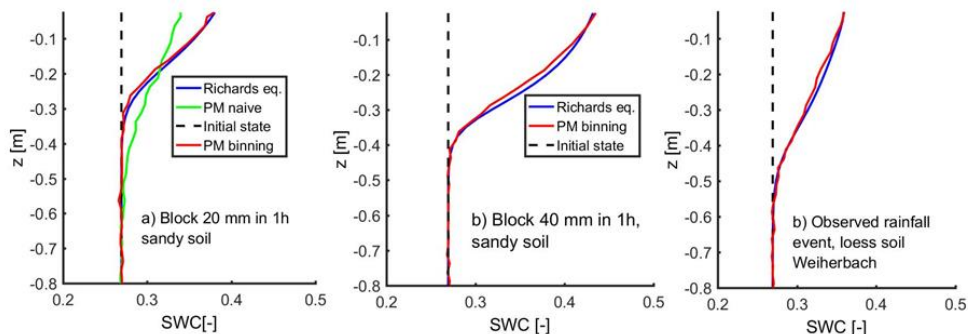
Figure A1. Soil moisture profiles simulated for **a)** a sandy soil and a block rain of 20 mm with a naive random walk (PM naive) and the Lagrangian particle model with binning (PM) according to Eq. 5 compared to a simulation with a Richards model, **b)** a sandy soil and a block rain of 40 mm, and **c)** an observed convective rainfall in the Weiherbach catchment (figure and caption are taken from Zehe and Jackisch (2016)).
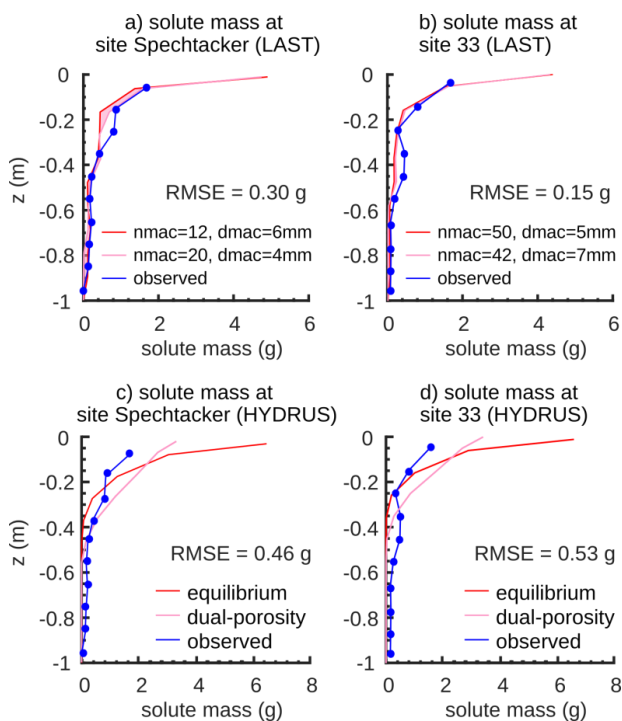
Figure A2. Simulated and observed bromide mass profiles at two study sites (Spechtacker, 33) in the Weiherbach catchment (a+b). Rose areas represent the standard deviation of observed macropore numbers (*nmac*) and diameters (*dmac*) from mean values at the sites. In comparison, simulated bromide mass profiles at the two sites simulated with HYDRUS 1-D (c+d). The rose and red profile are, respectively, simulated with a dual-porosity approach and an equilibrium approach (figure taken from Sternagel et al., 2019).

References

Ackermann, M.: Hydrogeologische Systemanalyse und Grundwasserhaushalt des Weiherbach-Einzugsgebietes, Lehrstuhl für Angewandte Geologie der Universität Karlsruhe, 1998.

5 Arias-Estévez, M., Lopez-Periago, E., Martinez-Carballo, E., Simal-Gandara, J., Mejuto, J. C., and Garcia-Rio, L.: The mobility and degradation of pesticides in soils and the pollution of groundwater resources, Agric. Ecosyst. Environ., 123, 247-260, 10.1016/j.agee.2007.07.011, 2008.

Bending, G. D., Shaw, E., and Walker, A.: Spatial heterogeneity in the metabolism and dynamics of isoproturon degrading microbial communities in soil, Biol. Fertil. Soils, 33, 484-489, 2001.

10 Bending, G. D., Lincoln, S. D., Sørensen, S. R., Morgan, J. A. W., Aamand, J., and Walker, A.: In-field spatial variability in the degradation of the phenyl-urea herbicide isoproturon is the result of interactions between degradative Sphingomonas spp. and soil pH, Appl. Environ. Microbiol., 69, 827-834, 2003.

Bending, G. D., and Rodriguez-Cruz, M. S.: Microbial aspects of the interaction between soil depth and biodegradation of the herbicide isoproturon, Chemosphere, 66, 664-671, 10.1016/j.chemosphere.2006.07.099,

15 2007.

Benson, D. A., Aquino, T., Bolster, D., Engdahl, N., Henri, C. V., and Fernandez-Garcia, D.: A comparison of Eulerian and Lagrangian transport and non-linear reaction algorithms, Adv. Water Resour., 99, 15-37, 2017.

Berkowitz, B., Cortis, A., Dentz, M., and Scher, H.: Modeling non-Fickian transport in geological formations as a continuous time random walk, Reviews of Geophysics, 44, 2006.

20 Berkowitz, B., Dror, I., Hansen, S. K., and Scher, H.: Measurements and models of reactive transport in geological media, Reviews of Geophysics, 54, 930-986, 2016.

Beven, K., and Germann, P.: Macropores and water flow in soils, Water resources research, 18, 1311-1325, 1982.

Beven, K., and Germann, P.: Macropores and water flow in soils revisited, Water Resources Research, 49, 3071-3092, 10.1002/wrcr.20156, 2013.

25 Binet, F., Kersanté, A., Munier-Lamy, C., Le Bayon, R.-C., Belgy, M.-J., and Shipitalo, M. J.: Lumbricid macrofauna alter atrazine mineralization and sorption in a silt loam soil, Soil Biology and Biochemistry, 38, 1255-1263, 2006.

Boivin, A., Cherrier, R., and Schiavon, M.: A comparison of five pesticides adsorption and desorption processes in thirteen contrasting field soils, Chemosphere, 61, 668-676, 2005.

30 Bolduan, R., and Zehe, E.: Degradation of isoproturon in earthworm macropores and subsoil matrix - a field study, Journal of Plant Nutrition and Soil Science, 169, 87-94, 10.1002/jpln.200521754, 2006.

Boso, F., Bellin, A., and Dumbser, M.: Numerical simulations of solute transport in highly heterogeneous formations: A comparison of alternative numerical schemes, Adv. Water Resour., 52, 178-189, 2013.

Bücker-Gittel, M., Mohrlok, U., and Jirka, G.: Modelling unsaturated water transport using a random walk

35 approach, IAHS PUBLICATION, 17-21, 2003.

Bundt, M., Widmer, F., Pesaro, M., Zeyer, J., and Blaser, P.: Preferential flow paths: biological 'hot spots' in soils, Soil Biology and Biochemistry, 33, 729-738, 2001.

Carter, A.: How pesticides get into water-and proposed reduction measures, Pesticide Outlook, 11, 149-156, 2000.

Clay, S. A., and Koskinen, W. C.: Effect of variability of soil properties as a function of depth on pesticide sorption-

40 desorption, in, ACS Publications, 2003.

Cui, Z., Welty, C., and Maxwell, R. M.: Modeling nitrogen transport and transformation in aquifers using a particle-tracking approach, Computers & Geosciences, 70, 1-14, 2014.

Davies, J., and Beven, K.: Comparison of a Multiple Interacting Pathways model with a classical kinematic wave subsurface flow solution, Hydrological Sciences Journal-Journal Des Sciences Hydrologiques, 57, 203-216, 10.1080/02626667.2011.645476, 2012.

de Jonge, L. W., Moldrup, P., Rubæk, G. H., Schelde, K., and Djurhuus, J.: Particle leaching and particle-facilitated transport of phosphorus at field scale, Vadose Zone Journal, 3, 462-470, 2004.

Dechesne, A., Badawi, N., Aamand, J., and Smets, B. F.: Fine scale spatial variability of microbial pesticide degradation in soil: scales, controlling factors, and implications, Frontiers in Microbiology, 5, 10.3389/fmicb.2014.00667, 2014.

Delay, F., and Bodin, J.: Time domain random walk method to simulate transport by advection-dispersion and matrix diffusion in fracture networks, Geophysical Research Letters, 28, 4051-4054, 10.1029/2001gl013698, 2001.

Dubus, I. G., Brown, C. D., and Beulke, S.: Sources of uncertainty in pesticide fate modelling, Sci. Total Environ., 317, 53-72, 2003.

Eilers, K. G., Debenport, S., Anderson, S., and Fierer, N.: Digging deeper to find unique microbial communities: The strong effect of depth on the structure of bacterial and archaeal communities in soil, Soil Biology & Biochemistry, 50, 58-65, 10.1016/j.soilbio.2012.03.011, 2012.

El-Sebai, T., Lagacherie, B., Cooper, J. F., Soulas, G., and Martin-Laurent, F.: Enhanced isoproturon mineralisation in a clay silt loam agricultural soil, Agronomy for Sustainable Development, 25, 271-277, 10.1051/agro:2005003, 2005.

Engdahl, N. B., Benson, D. A., and Bolster, D.: Lagrangian simulation of mixing and reactions in complex geochemical systems, Water Resources Research, 53, 3513-3522, 2017.

Engdahl, N. B., Schmidt, M. J., and Benson, D. A.: Accelerating and Parallelizing Lagrangian Simulations of Mixing-Limited Reactive Transport, Water Resources Research, 55, 3556-3566, 2019.

Ewen, J.: 'SAMP' model for water and solute movement in unsaturated porous media involving thermodynamic subsystems and moving packets .1. Theory, Journal Of Hydrology, 182, 175-194, 10.1016/0022-1694(95)02925-7, 1996a.

Ewen, J.: 'SAMP' model for water and solute movement in unsaturated porous media involving thermodynamic subsystems and moving packets .2. Design and application, Journal Of Hydrology, 182, 195-207, 10.1016/0022-1694(95)02926-5, 1996b.

Farenhorst, A.: Importance of soil organic matter fractions in soil-landscape and regional assessments of pesticide sorption and leaching in soil, Soil Sci. Soc. Am. J., 70, 1005-1012, 2006.

Flury, M.: Experimental evidence of transport of pesticides through field soils - A review, Journal Of Environmental Quality, 25, 25-45, 1996.

Fomsgaard, I. S.: Degradation of pesticides in subsurface soils, unsaturated zone—a review of methods and results, International Journal of Environmental Analytical Chemistry, 58, 231-245, 1995.

Frey, M. P., Schneider, M. K., Dietzel, A., Reichert, P., and Stamm, C.: Predicting critical source areas for diffuse herbicide losses to surface waters: Role of connectivity and boundary conditions, Journal of Hydrology, 365, 23-36, 10.1016/j.jhydrol.2008.11.015, 2009.

Gassmann, M., Stamm, C., Olsson, O., Lange, J., Kümmerer, K., and Weiler, M.: Model-based estimation of pesticides and transformation products and their export pathways in a headwater catchment, Hydrol. Earth Syst. Sci., 17, 5213-5228, 10.5194/hess-17-5213-2013, 2013.

Gerke, H. H., and van Genuchten, M. T.: A Dual-Porosity Model for Simulating the Preferential Movement of
5   Water and Solutes in Structured Porous-Media, Water Resources Research, 29, 305-319, 1993.

Gerke, H. H.: Preferential flow descriptions for structured soils, Journal of Plant Nutrition and Soil Science, 169, 382-400, 10.1002/jpln.200521955, 2006.

Gill, H. K., and Garg, H.: Pesticide: environmental impacts and management strategies, Pesticides-toxic aspects, 8, 187, 2014.

10   Green, C. T., LaBolle, E. M., Fogg, G. E., and Davis, C.: Random walk particle tracking for simulating reactive transport in heterogeneous aquifers: effects of concentraction averaging, Proceedings of the International Groundwater Symposium. International Association of Hydraulic Research and American Geophysical Union, Berkeley, CA, 2002,

Hansen, S. K., and Berkowitz, B.: Modeling Non-Fickian Solute Transport Due to Mass Transfer and Physical
15   Heterogeneity on Arbitrary Groundwater Velocity Fields, Water Resources Research, 56, e2019WR026868, 10.1029/2019wr026868, 2020.

Haws, N. W., Rao, P. S. C., Simunek, J., and Poyer, I. C.: Single-porosity and dual-porosity modeling of water flow and solute transport in subsurface-drained fields using effective field-scale parameters, Journal of Hydrology, 313, 257-273, 10.1016/j.jhydrol.2005.03.035|ISSN 0022-1694, 2005.

20   Holden, P. A., and Fierer, N.: Microbial processes in the vadose zone, Vadose Zone Journal, 4, 1-21, 2005.

Jackisch, C., and Zehe, E.: Ecohydrological particle model based on representative domains, Hydrology And Earth System Sciences, 22, 3639-3662, 10.5194/hess-22-3639-2018, 2018.

Jarvis, N., and Larsbo, M.: MACRO (v5.2): Model Use, Calibration, and Validation, Trans. ASABE, 55, 1413-1423, 2012.

25   Jensen, P. H., Hansen, H. C. B., Rasmussen, J., and Jacobsen, O. S.: Sorption-controlled degradation kinetics of MCPA in soil, Environmental science & technology, 38, 6662-6668, 2004.

Klaus, J., and Zehe, E.: Modelling rapid flow response of a tile drained field site using a 2D-physically based model: assessment of "equifinal" model setups, Hydrological Processes, 24, 1595 – 1609, DOI: 10.1002/hyp.7687., 2010.

30   Klaus, J., and Zehe, E.: A novel explicit approach to model bromide and pesticide transport in connected soil structures, Hydrology And Earth System Sciences, 15, 2127-2144, 10.5194/hess-15-2127-2011, 2011.

Klaus, J., Zehe, E., Elsner, M., Kulls, C., and McDonnell, J. J.: Macropore flow of old water revisited: experimental insights from a tile-drained hillslope, Hydrology And Earth System Sciences, 17, 103-118, 10.5194/hess-17-103-2013, 2013.

35   Klaus, J., Zehe, E., Elsner, M., Palm, J., Schneider, D., Schroeder, B., Steinbeiss, S., van Schaik, L., and West, S.: Controls of event-based pesticide leaching in natural soils: A systematic study based on replicated field scale irrigation experiments, Journal Of Hydrology, 512, 528-539, 10.1016/j.jhydrol.2014.03.020, 2014.

Knabner, P., Totsche, K., and Kögel-Knabner, I.: The modeling of reactive solute transport with sorption to mobile and immobile sorbents: 1. Experimental evidence and model development, Water Resources Research, 32, 1611-
40   1622, 1996.

Köhne, J. M., Köhne, S., and Šimůnek, J.: A review of model applications for structured soils: a) Water flow and tracer transport, Journal of Contaminant Hydrology, 104, 4-35, 10.1016/j.jconhyd.2008.10.002, 2009a.

Köhne, J. M., Köhne, S., and Šimůnek, J.: A review of model applications for structured soils: b) Pesticide transport, Journal of Contaminant Hydrology, 104, 36-60, http://dx.doi.org/10.1016/j.jconhyd.2008.10.003, 2009b.

Koutsoyiannis, D.: HESS Opinions" A random walk on water", Hydrology and Earth System Sciences, 14, 585-601, 2010.

Kutílek, M., and Nielsen, D. R.: Soil hydrology: texbook for students of soil science, agriculture, forestry, geoecology, hydrology, geomorphology and other related disciplines, Catena Verlag, 1994.

Leistra, M.: A model for the transport of pesticides in soil with diffusion-controlled rates of adsorption and desorption, Agriculture and Environment, 3, 325-335, 1977.

Lewis, K. A., Tzilivakis, J., Warner, D. J., and Green, A.: An international database for pesticide risk assessments and management, Human and Ecological Risk Assessment: An International Journal, 22, 1050-1064, 2016.

Liess, M., Schulz, R., Liess, M. H. D., Rother, B., and Kreuzig, R.: Determination of insecticide contamination in agricultural headwater streams, Water Research, 33, 239-247, 10.1016/s0043-1354(98)00174-2, 1999.

Liu, Y.-J., Zaprasis, A., Liu, S.-J., Drake, H. L., and Horn, M. A.: The earthworm Aporrectodea caliginosa stimulates abundance and activity of phenoxyalkanoic acid herbicide degraders, The ISME Journal, 5, 473-485, 10.1038/ismej.2010.140, 2011.

Loritz, R., Hassler, S. K., Jackisch, C., Allroggen, N., van Schaik, L., Wienhöfer, J., and Zehe, E.: Picturing and modeling catchments by representative hillslopes, Hydrol. Earth Syst. Sci., 21, 1225-1249, 10.5194/hess-21-1225-2017, 2017.

Mälicke, M. and Sternagel, A.: Code of the LAST-Model, Version 0.1.1, available at: https://github.com/KIT-HYD/last-model, last access: 12 October 2020.

Pimentel, D., Acquay, H., Biltonen, M., Rice, P., Silva, M., Nelson, J., Lipner, V., Giordano, S., Horowitz, A., and D'amore, M.: Environmental and economic costs of pesticide use, BioScience, 42, 750-760, 1992.

Plate, E., and Zehe, E.: Hydrologie und Stoffdynamik kleiner Einzugsgebiete: Prozesse und Modelle, Schweizerbart'sche Verlagsbuchhandlung (Nägele u. Obermiller), 366 pp., 2008.

Radcliffe, D., and Simunek, J.: Soil Physics with HYDRUS: Modeling and Applications, 20 CRC Press, New York, 2010.

Risken, H.: The Fokker-Planck Equation, Springer, Berlin 1984, 1984.

Rodríguez-Cruz, M. S., Jones, J. E., and Bending, G. D.: Field-scale study of the variability in pesticide biodegradation with soil depth and its relationship with soil characteristics, Soil Biology and Biochemistry, 38, 2910-2918, 2006.

Sander, T., and Gerke, H. H.: Modelling field-data of preferential flow in paddy soil induced by earthworm burrows, Journal of Contaminant Hydrology, 104, 126-136, 10.1016/j.jconhyd.2008.11.003, 2009.

Sarkar, B., Mukhopadhyay, R., Mandal, A., Mandal, S., Vithanage, M., and Biswas, J. K.: Sorption and desorption of agro-pesticides in soils, in: Agrochemicals Detection, Treatment and Remediation, Elsevier, 189-205, 2020.

Schmidt, M. J., Pankavich, S. D., Navarre-Sitchler, A., and Benson, D. A.: A Lagrangian method for reactive transport with solid/aqueous chemical phase interaction, Journal of Computational Physics: X, 2, 100021, 2019.

Simunek, J., van Genuchten, M. T., and Sejna, M.: Development and applications of the HYDRUS and STANMOD software packages and related codes, Vadose Zone Journal, 7, 587-600, 10.2136/vzj2007.0077, 2008.

Šimůnek, J., Jarvis, N. J., van Genuchten, M. T., and Gärdenäs, A.: Review and Comparison of models for describing non-equilibrium and preferential flow and transport in the vadose zone, Journal of Hydrology, 272, 14-35, 2003.

Sternagel, A., Loritz, R., Wilcke, W., and Zehe, E.: Simulating preferential soil water flow and tracer transport using the Lagrangian Soil Water and Solute Transport Model, Hydrology And Earth System Sciences, 23, 4249-4267, 10.5194/hess-23-4249-2019, 2019.

Tang, Q., Zhao, Z. P., Liu, Y. J., Wang, N. X., Wang, B. J., Wang, Y. N., Zhou, N. Y., and Liu, S. J.: Augmentation of tribenuron methyl removal from polluted soil with Bacillus sp strain BS2 and indigenous earthworms, J. Environ. Sci., 24, 1492-1497, 10.1016/s1001-0742(11)60947-9, 2012.

van Schaik, L., Palm, J., Klaus, J., Zehe, E., and Schroeder, B.: Linking spatial earthworm distribution to macropore numbers and hydrological effectiveness, Ecohydrology, 7, 401-408, 10.1002/eco.1358, 2014.

Villholth, K. G., Jarvis, N. J., Jacobsen, O. H., and de Jonge, H.: Field investigations and modeling of particle-facilitated pesticide transport in macroporous soil, Journal of Environmental Quality, 29, 1298-1309, 2000.

Wienhöfer, J., and Zehe, E.: Predicting subsurface stormflow response of a forested hillslope – the role of connected flow paths, Hydrology and Earth System Sciences, 18, 121-138, 10.5194/hess-18-121-2014, 2014.

Working Group WRB, I.: World Reference Base for Soil Resources 2014, International Soil Classification System for Naming Soils and Creating Legends for Soil Maps, World Soil Resources Reports No. 106, 2014.

Zehe, E.: Stofftransport in der ungesättigten Bodenzone auf verschiedenen Skalen, Institut für Hydrologie und Wasserwirtschaft, Mitteilungen des Instituts für Hydrologie und Wasserwirtschaft, Universität Karlsruhe (TH), Karlsruhe, 227 pp., 1999.

Zehe, E., and Flühler, H.: Preferential transport of isoproturon at a plot scale and a field scale tile-drained site, Journal of Hydrology, 247, 100-115, 2001.

Zehe, E., Maurer, T., Ihringer, J., and Plate, E.: Modeling water flow and mass transport in a loess catchment, Phys. Chem. Earth Pt B-Hydrol. Oceans Atmos., 26, 487-507, 2001.

Zehe, E., and Blöschl, G.: Predictability of hydrologic response at the plot and catchment scales: Role of initial conditions, Water Resources Research, 40, W10202 10.1029/2003wr002869, 2004.

Zehe, E., and Jackisch, C.: A Lagrangian model for soil water dynamics during rainfall-driven conditions, Hydrology And Earth System Sciences, 20, 3511-3526, 10.5194/hess-20-3511-2016, 2016.